*Pure Appl. Chem.*, Vol. 76, No. 9, pp. 1715–1734, 2004.


# Superheavy elements*

Yury Ts. Oganessian‡

*Flerov Laboratory of Nuclear Reactions, Joint Institute for Nuclear Research, 141980 Dubna, Moscow, Russia*

*Abstract*: One of the fundamental outcomes of nuclear theory is the predicted existence of increased stability in the region of unknown superheavy elements. This hypothesis, proposed more than 35 years ago and intensively developed during all this time, significantly extends the limits of existence of chemical elements. "Magic" nuclei with closed proton and neutron shells possess maximum binding energy. For the heaviest nuclides, a considerable stability is predicted close to the deformed shells with $Z = 108$, $N = 162$. Even higher stability is expected for the neutron-rich nuclei close to the spherical shells with $Z = 114$ (possibly also at $Z = 120$, 122) and $N = 184$, coming next to the well-known "doubly magic" nucleus $^{208}$Pb. The present paper describes the experiments aimed at the synthesis of nuclides with $Z = 113$–116, 118 and $N = 170$–177, produced in the fusion reactions of the heavy isotopes of Pu, Am, Cm, and Cf with $^{48}$Ca projectiles. The energies and half-lives of the new nuclides, as well as those of their daughter nuclei ($Z < 113$) qualitatively agree with the theoretical predictions. The question, which is the nucleus, among the superheavy ones, that has the longest half-life is also considered. It has been shown that, if the lifetime of the most stable isotopes, in particular, the isotopes of element 108 (Hs), is $\geq 5 \times 10^7$ years, they can be found in natural objects. The experiments were carried out during 2001–2003 in the Flerov Laboratory of Nuclear Reactions (JINR, Dubna) in collaboration with the Analytical and Nuclear Chemistry Division (LLNL, Livermore).

## INTRODUCTION

According to the quantum electrodynamics (QED) theory, the well-known concept of the atom as a system consisting of a nucleus, carrying almost entirely the atomic mass, and electron orbits, lying at a large distance from the charge center, is valid for very heavy atoms ($Z \sim 170$ or even more). Nevertheless, the limit of existence of atoms (elements) is reached much earlier because of the instability of the nucleus itself.

It is well known that changes in the proton-to-neutron ratio in the nucleus generate β-decay. An excess of neutrons in a nucleus leads to the reduction of the neutron binding energy; the limit is reached at $E_n = 0$ (the neutron drip line). Similarly, zero proton binding energy, $E_p = 0$ (the proton drip line), determines the boundary of existence of proton-rich nuclei. Another boundary is associated with the maximum possible number of nucleons in the nucleus. Formally, the limiting mass of the nucleus is determined by the probability of its division into parts of smaller masses. For the first time in 1940, this type of nuclear transformations, viz., the spontaneous fission (SF) of heavy nuclei, was observed for the isotope $^{238}$U ($T_{SF} = 10^{16}$ yr) by Flerov and Petrzhak [1].

By that time, Hahn and Strassman had already discovered the induced fission of uranium. In order to describe this phenomenon, Bohr and Wheeler proposed the liquid-drop model of nuclear fission [2].

---

*Plenary lecture presented at the XVII Mendeleev Congress on General and Applied Chemistry, Kazan, Tatarstan, Russia, 21–26 September 2003. Other presentations are published in this issue, pp. 1605–1798.

‡E-mail: oganessian@flnr.jinr.ru

This beautiful theoretical model, which is essentially classical, is based on the assumption that nuclear matter is an amorphous (structureless) matter similar to a drop of charged liquid. A deformation of the drop due to Coulomb forces eventually arises upon overcoming the potential barrier, which tends to hinder the deformation of the nucleus. For the $^{238}$U nucleus, the height of the fission barrier is $B_f \approx 6$ MeV. With increasing $Z$, the height of the fission barrier decreases fast; as a result, at some critical value of the nuclear charge, the nucleus becomes absolutely unstable with respect to spontaneous fission ($T_{SF} \sim 10^{-19}$ s). According to the estimates of Bohr and Wheeler, this critical situation is realized as soon as the charge number reaches values of $Z \sim 106$.

The discovery of isomers that can undergo spontaneous fission [3,4] was unexpected insofar as it was at odds with the liquid-drop model. It has been shown that the shape isomerism in the well-known 33 nuclei (isotopes of nuclei occurring between U and Cm) is due to the complicated shape of the nuclear potential-energy surface, in particular, to the two-humped shape of their fission barrier. Yet another contradiction to theory was revealed in the considerable variations of the spontaneous fission half-lives with small change of proton or neutron number that was observed in the isotopes of Cf and Fm, as well as in the isotopes of transfermium elements formed in heavy-ion reactions [5].

A more detailed analysis of the theoretical and experimental values of nuclear masses has shown that the deviations of the experimental nuclear binding energies from the theoretical ones behave quite regularly: they are maximal (highest binding energy) at specific magic numbers of protons and neutrons in a nucleus. Calculations performed within the macroscopic–microscopic model revealed regular shell phenomena and thus improved substantially the accuracy in predicting their ground-state masses and shapes.

## NUCLEAR SHELLS AND STABILITY OF HEAVY ELEMENTS

Like any theory, the model being discussed possessed some predictive power, for example, in dealing with very heavy, hitherto unknown nuclei. Predictions on its basis were made in a number of studies. Here, we present the results of Patyk and Sobiczewski [6] and Smolanczuk [7], who computed the masses and the fission barriers of even–even nuclei with $Z = 104$–$120$ and $N = 140$–$190$.

Let us first dwell at some length on the probabilities of spontaneous fission of superheavy nuclei. The liquid-drop fission barrier is nearly zero for the heavy nucleus $^{270}$108. Upon the inclusion of the shell correction in the calculation of the nuclear potential energy, the above-mentioned nuclei develop fission barriers of height of about 6–8 MeV. The onset of a potential barrier, when a heavy nucleus is deformed, is expected to severely suppress spontaneous fission. Indeed, it follows from the theoretical results displayed in Fig. 1a that the partial half-lives with respect to spontaneous fission depend greatly on the amplitude of the shell correction. The considerable growth of $T_{SF}(N)$ for nuclei that recede from the $N = 152$ shell, which manifests itself clearly in the radioactive properties of the actinide nuclei, is associated with the effect of another neutron shell, that with $N = 162$. It should be noted that either shell is associated with deformed nuclei. The highest stability with respect to spontaneous fission is expected for the $^{270}$108 ($N = 162$) nucleus; the $T_{SF}$ value predicted for this nuclide can be as large as a few hours. With an increasing number of neutrons, the nuclear deformation becomes less pronounced because, in that case, we move away from the $N = 162$ shell, which is deformed, and because another closed spherical shell, that with $N = 184$, comes into play. For $N > 170$, it is natural to expect a significant growth of $T_{SF}(N)$ persisting up to the $^{292}$108 ($N = 184$) nucleus, whose partial half-life with respect to spontaneous fission is $T_{SF} \sim 3 \times 10^4$ yr, an enormous value indeed.

Here, we come across a very interesting situation. If superheavy nuclei possess high stability with respect to spontaneous fission, they will decay through other modes, such as alpha decay and, possibly, beta decay. The probability of these decay modes and, hence, the corresponding lifetimes will be determined by the ground-state nuclear masses. As can be seen in Fig. 1b, the effect of the nuclear shells

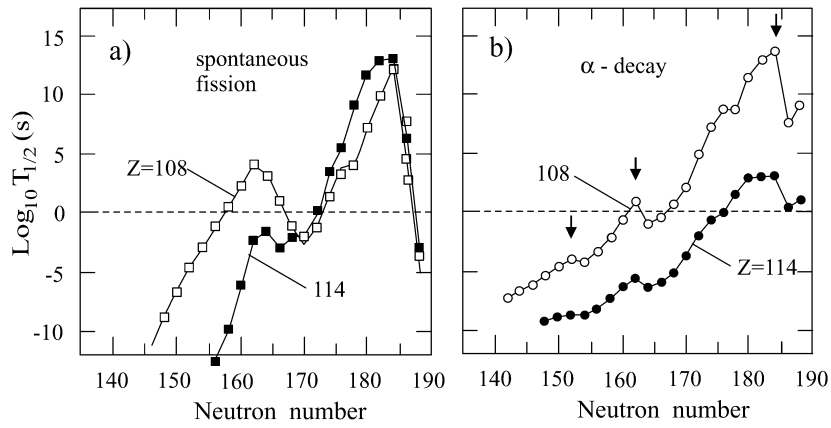


**Fig. 1** Partial half-lives with respect: (a) to the spontaneous fission and (b) to the α-decay of even–even isotopes with $Z$ = 108 and 114 containing various numbers of neutrons. The arrows indicate the neutron numbers corresponding to the closed shells with $N$ = 152, 162, and 184.

leads to a considerable rise in $T_\alpha$. At the same time, the proton-to-neutron ratio in these nuclides places them close to the β-stability line.

Therefore, it becomes possible to draw the fundamental conclusion that islands of stability can exist in the region of very heavy nuclei and thus the limits of existence of elements can be significantly extended.

## SYNTHESIS REACTIONS

It is well known that the first man-made elements heavier than uranium were synthesized in reactions of successive neutron captures during long-term exposures at high-flux nuclear reactors. The long lifetimes of the new nuclides made it possible to separate and identify them by radiochemical methods followed by the measurement of their radioactive-decay properties. These pioneering studies performed by Prof. G. T. Seaborg and his colleagues between 1940 and 1953 at the Lawrence Berkeley National Laboratory (for an overview, see, e.g., [8]) resulted in the discovery of eight man-made elements with $Z$ = 93–100, the heaviest isotope being $^{257}$Fm ($T_{1/2}$ ~ 100 d). The further advancement toward the region of heavier nuclei was hindered by the extremely small lifetime of $^{258}$Fm ($T_{SF}$ = 0.3 ms). Attempts to overcome this barrier in pulsed high-intensity neutron fluxes from underground nuclear explosions did not produce anything beyond $^{257}$Fm.

Transfermium elements with masses $A > 257$ were produced in heavy-ion reactions. In contrast to (n, γ) reactions, where the excitation energy of the nucleus is 6–8 MeV, the fusion reactions involving an ion as light as $^4$He are already characterized by $E_x^{min}$ = 20 MeV. With increasing the projectile-ion mass, the excitation energy of the compound nucleus increases due to the growth of the Coulomb barrier. The transition of a hot nucleus to the ground state ($E_x = 0$) will proceed predominantly through the emission of neutrons and gamma rays.

However, as a result of the high fissility of the hot nucleus, the survival ability of evaporation products decreases fast with increasing $E_x$ (this is equivalent to an increase in the number of neutron-evaporation cascades). The situation is aggravated by the fact that the shell effect, which suppresses the fission of a nucleus in the ground state, decreases fast with increasing excitation energy. Both these factors lead to an extremely small survival probability of heavy compound nuclei.

The advent into the region of heavier elements with $Z > 106$ became possible after the discovery of the so-called "cold-fusion" reactions, where $^{208}$Pb or $^{209}$Bi are used as target material, while ions with $A > 40$ are used as projectiles [9]. In these reactions, the increase of the Coulomb barrier is com-

pensated by the nuclear mass excess—similarly to the reactions of "inverse fission", as a result of which the compound nucleus has a low excitation energy ($E_x$ ~ 12–18 MeV). The "cold-fusion" reactions allowed synthesizing the elements with $Z$ = 107–112. Unfortunately, due to the hindrance to fusion of massive nuclei, which grows with the increase of the ion mass, the probability of forming new elements exponentially falls when increasing the compound nucleus atomic number $Z$. In going from element 102 (the reaction $^{208}$Pb + $^{48}$Ca) to element 112 ($^{208}$Pb + $^{70}$Zn), it turns out that the probability of producing the new element drops by a factor of more than $10^6$.

At the same time, this is not the main obstacle standing on the way of synthesis of new elements. The compound nuclei, produced in cold-fusion reactions, contain a relatively small number of neutrons. In the above-mentioned case of producing element 112, the final nucleus with $Z$ = 112 has only 165 neutrons, while the increase of stability is expected for neutron number $N$ > 170 (see Fig. 1).

Nuclides with so high a neutron excess can in principle be obtained by using heavy actinide isotopes with $Z$ = 94–98 as the target material and nuclei of the rare isotope $^{48}$Ca as projectiles.

Because of the considerable mass defect in the doubly magic nucleus $^{48}$Ca, the excitation energy of the compound nucleus above the Coulomb barrier is about 30 MeV. The cooling of the nucleus occurs via the emission of three neutrons and gamma rays. It can be expected that, at this excitation energy, shell effects are still noticeable and the probability of survival of evaporation products is larger than in the case of hot-fusion reactions ($E_x \geq 50$ MeV). At the same time, the mass asymmetry in the entrance channel ($Z_1 \times Z_2 \leq 2000$) should reduce the dynamical suppression of fusion of the nuclei being considered and, hence, increase the cross-section for compound-nucleus formation relative to that of cold-fusion reactions.

Despite these obvious advantages, all the preceding attempts made between 1977 and 1985 at various laboratories [11–13] to synthesize new elements yielded only upper limits on the cross-sections for the formation of superheavy elements. However, the progress in experimental techniques over the recent years and the possibility of obtaining intense beams of $^{48}$Ca ions at new-generation heavy-ion accelerators make it possible to improve the sensitivity of relevant experiments by two or even three orders of magnitude. We have, therefore, chosen this way to advance toward the region of stability of superheavy elements.

## EXPERIMENTAL TECHNIQUE

The technique of our experiments on the synthesis of superheavy elements (SHEs) with the $^{48}$Ca ion beam has been described elsewhere [14]. Here, we give only a few details considering the experimental setup and methods.

The beam of $^{48}$Ca with an intensity of about 1.5 pμA hits a rotating target that consists of a thin (0.35 mg/cm$^2$) layer of Pu, Cm, or Cf oxides on a 1.5-μm-thick titanium backing.

In the present experiments, the compound nuclei recoiling from the target were separated in flight from the $^{48}$Ca-beam ions, scattered particles and transfer-reaction products by the Dubna Gas-Filled Recoil Separator (Fig. 2). The transmission efficiency of the separator for $Z$ = 114 and 116 nuclei was estimated to be about 35–40 %. The separator was operated with hydrogen filling at a pressure of about 1 Torr.

Evaporation recoils pass through a time-of-flight (TOF) system and are implanted in a 4 × 12-cm$^2$ semiconductor front detector with 12 vertical position-sensitive strips, located in the separator's focal plane, 4 m downstream the target. This detector is surrounded by eight 4 × 4-cm$^2$ side detectors without position sensitivity, forming a box of detectors open from the coming-beam side. The position-averaged detection efficiency for α-decays of implanted nuclei is 87 % of 4$\pi$. Single SF fragments are detected with 100 % efficiency, and coincident pairs of fission fragments (front and side detectors) are detected with about 40 % efficiency. The energy resolution for α-particles absorbed in the front detector is 60–90 keV. Alpha-particles escaping at different angles and registered by the front and side detectors have energy resolution of the summed signals of 140–200 keV. The full width at half-maximum

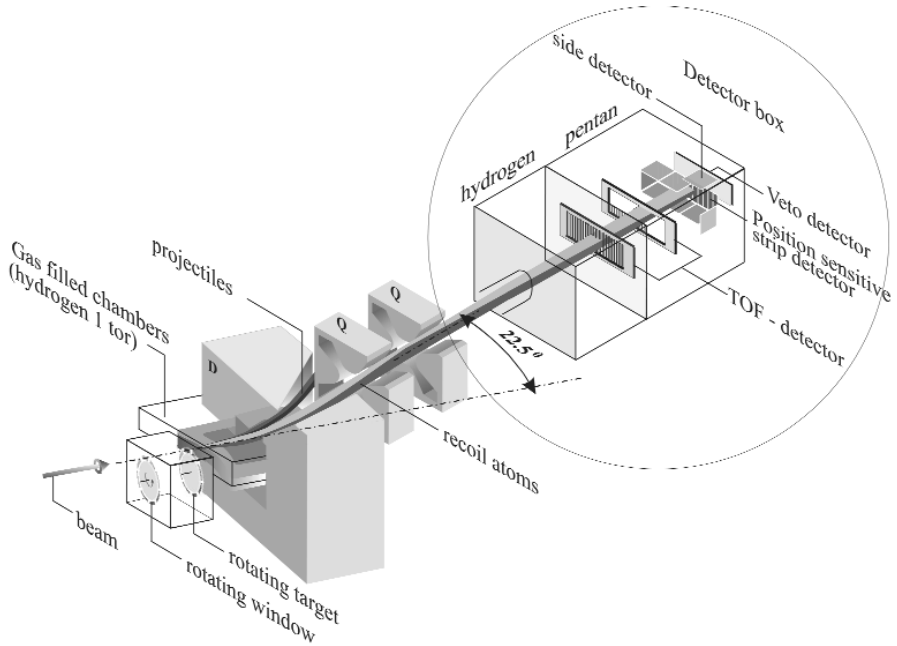


**Fig. 2** A schematic view of the Dubna Gas-Filled Recoil Separator.

(FWHM) position resolution of the signals of correlated decays of nuclei implanted in the detectors are 0.8–1.3 mm for R-α signals and 0.5–0.8 mm for R-SF signals.

In the position-sensitive strips, detector signals from implanted recoils should be accompanied by TOF signals. Signals from the decay of implanted nuclei have no TOF mark. Sequences of genetically linked decays (e.g., R-α-α…SF) are characterized by coordinates (strip number and position on strip) that coincide within the detector position resolution. In identical decay sequences, the α-particle energies measured for the corresponding members of the decay chains should also coincide within the detector energy resolution and the distribution of decay times should correspond to the exponential radioactive decay law.

In many experiments, we used a special detection mode for registering two or more sequential decays. The beam was switched off after a recoil signal was detected with parameters of implantation energy and TOF expected for the evaporation residues, followed by an α-like signal within a preset energy and time interval, in the same strip, within a position window of about 1.5 mm. In this way, all the expected sequential decays of the daughter nuclides should be observed in the absence of beam-associated background. Such a technique appeared to be especially efficient in detecting long-lived multistep decay chains like those we obtained in our experiments on the synthesis of elements 115 and 113.

## SYNTHESIS OF ISOTOPES OF ELEMENTS 114 AND 116 IN THE REACTIONS $^{244}$Pu AND $^{248}$Cm + $^{48}$Ca

The first experiments of 1998–1999 that aimed at the synthesis of the isotopes of element 114 in the reaction $^{244}$Pu + $^{48}$Ca were performed with the beam energy of 236 MeV, which corresponds to the excitation energy of the compound nucleus $^{292}$114, $E_x$ ~ 36 MeV [15]. Accordingly, one could expect 3*n*- and 4*n*-evaporation to be the most probable reaction channels, which lead to the isotopes $^{288,289}$114. The two events shown in Fig. 3a illustrate the observations. In both R-$\alpha_1$-$\alpha_2$-SF decay chains detected in strips 2 and 8, all four decays have positions that differ by not more than 0.6 mm. The measured decay energies and times meet all the criteria stated above. In further experiments, three more events of

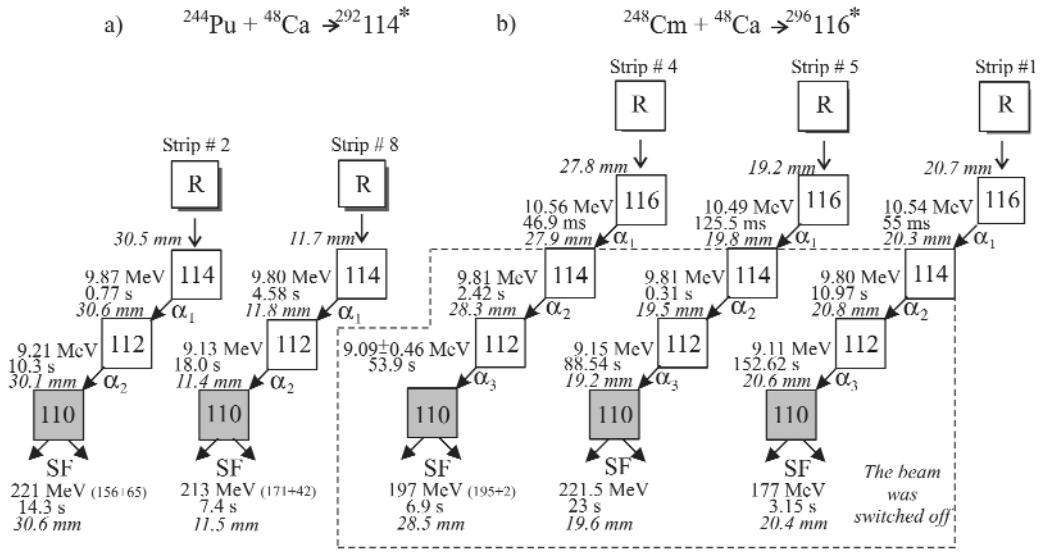


**Fig. 3** Decay chains observed in the reactions: (a) $^{244}Pu + ^{48}Ca$; (b) $^{248}Cm + ^{48}Ca$. The measured energies (in MeV), the time of emission of α-particles, and the coordinate defining their position on the strip are given for each α-decay. The same parameters are shown also for the SF events. In the case of registering two fission fragments, the values of the sum and the individual energy signals are shown for each fission fragment (in brackets).

the same type were detected. The decay pattern, as well as the decay energies and times in the observed decay sequences, are close to what could be expected for isotopes of element 114 with $N = 174–175$.

In order to verify this assignment we performed another experiment with a $^{248}Cm$ target [16]. In this case, the reaction leads to the production of the isotopes of element 116. Following the α-decay of the mother nucleus, its daughter products, i.e., the isotopes of elements 114, 112, and 110, should reproduce the decay pattern observed in the reaction $^{244}Pu + ^{48}Ca$. In other words, the mother nucleus obtained in the $^{244}Pu + ^{48}Ca$ reaction becomes the α-decay daughter of the heavier nucleus with $Z = 116$ that was produced in the reaction with the $^{248}Cm$ target.

The decay chains presented in Fig. 3b show the complete coincidence of the decay characteristics of the nuclides with $Z = 114$, 112, and 110 observed in both reactions. From the three events observed, we obtain that the isotope of element 116 undergoes α-decay with $E_\alpha = 10.53$ MeV and $T_\alpha \sim 53$ ms. Three decay events of its daughter with $Z = 114$ agree with the five events detected in the reaction $^{244}Pu + ^{48}Ca$, $E_\alpha = 9.82$ MeV, $T_\alpha \sim 2.7$ s. All eight decays referring to $Z = 112$ show $E_\alpha = 9.16$ MeV and $T_\alpha \sim 35$ s. Finally, in eight cases, also the final nucleus with $Z = 110$ decays by spontaneous fission with $T_{SF} \sim 9.6$ s and is characterized by a high value of the fission fragments energy released in the detectors, $E_{tot} \sim 205$ MeV. If one takes into account the loss of the kinetic energy of fission fragments in the dead layers of the detection system ($\Delta E_{tot} \sim 25$ MeV as it was for the SF of $^{252}No$), the measured value corresponds to a total kinetic energy (TKE) ~ 230 MeV. The latter value exceeds the TKE of 180 MeV typical for SF of $^{252}Cf$ by some 50 MeV and also gives evidence for the fission of a heavy nuclide (see below).

The α-particle energy spectrum presented in Fig. 4a shows the well-defined energy of all the three α-decays in the decay chain $Z = 116–114–112–110$, which points to the decay via unhindered α-transitions. In the absence of hindrance, the α-decay energy $Q_\alpha$ and the decay probability (or the half-life $T_\alpha$) are known to follow the Geiger–Nuttal relation ($\mathrm{Log}T_\alpha \sim Z \times Q_\alpha^{-1/2}$). This relation, in the form of the Viola–Seaborg formula [17], is fulfilled quite well for the 60 known even–even nuclides with $Z > 82$ for which the α-decay energies and half-lives have been measured. In Fig. 5, the black points show the data obtained in the experiments $^{244}Pu,^{248}Cm + ^{48}Ca$. Using the relationship $\mathrm{Log}T_\alpha$ vs. ($Q_\alpha$), the

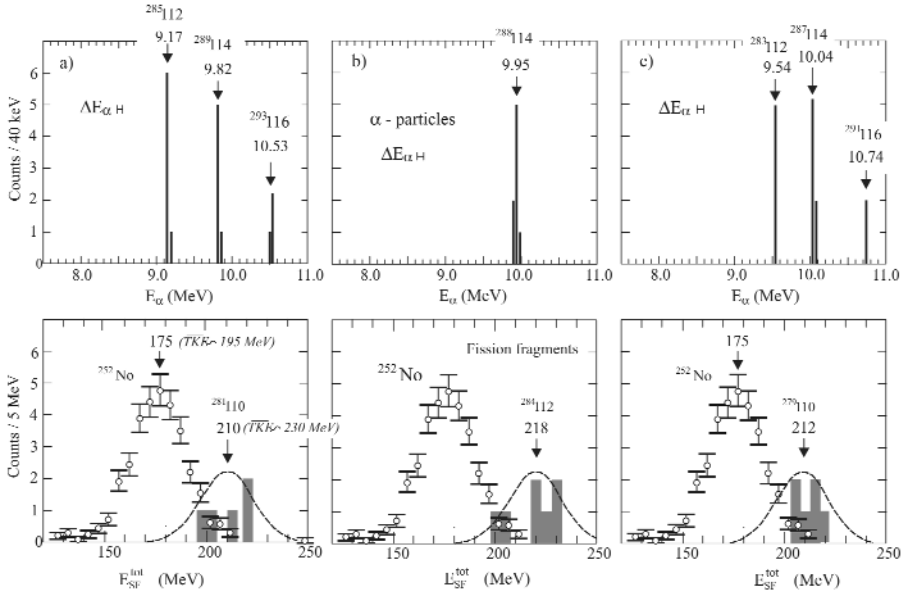


**Fig. 4** Energy spectra of the α-particles and of the sum energy of SF fragment pairs measured in various decay chains: (a) α-α-SF chain in the reaction $^{244}$Pu($^{48}$Ca, 3*n*)$^{289}$114 and α-α-α-SF chain in the reaction $^{248}$Cm($^{48}$Ca, 3*n*)$^{293}$116; (b) α-SF chain in the reaction $^{244}$Pu($^{48}$Ca, 4*n*)$^{288}$114; (c) α-α-SF chain in the reaction $^{244}$Pu($^{48}$Ca, 5*n*)$^{287}$114 and α-α-α-SF chain in the reaction $^{245}$Cm($^{48}$Ca, 2*n*)$^{291}$116. The lower plots show the sum energies of the SF fragment pairs measured by the detector array. Dots show the spectrum of the fragments of the SF of $^{252}$No produced in the reaction $^{206}$Pb($^{48}$Ca, 2*n*).

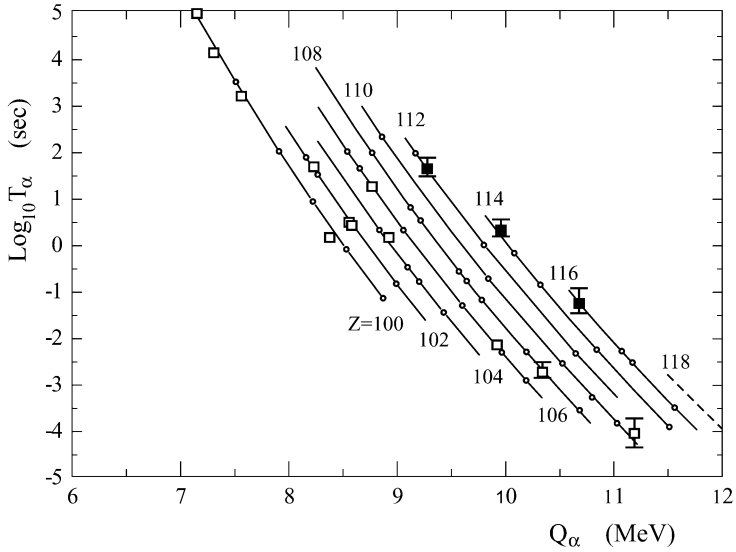


**Fig. 5** Dependence of Log($T_\alpha$) vs. $(Q_\alpha)^{-1/2}$ for the α-decay of even-*Z* nuclei with *Z* = 100–118. Open squares show experimental data for the isotopes with *Z* = 100–110. Full squares refer to the decay of the isotopes of elements 116–114–112 produced in the reactions $^{244}$Pu, $^{248}$Cm + $^{48}$Ca. Lines present the values calculated with the Viola–Seaborg formula [17].

$Z$ value for every decay in the observed α-α-α-SF sequence can be calculated. Taking into account the genetic correlation of the three decays, one can estimate the probability that the observed sequential decays refer to the nuclei with $Z$ = 116–114–112. This value exceeds 99.2 %. Thus, the probability of missing the first α-particle and that the decays refer to the chain with $Z$ = 114–112–110 is less than 0.8 %.

Unfortunately, the definite mass-identification of the new nuclide is problematic. In the domain of the neutron-rich nuclei under consideration, the decay chains start from and end in nuclides with unknown decay properties. Thus, the widely used method of genetic correlations to known nuclei for the identification of the parent nuclide has a limited application.

In our case, for the mass-identification one needs to determine the number of neutrons emitted by the excited compound nucleus. The energy dependence of the cross-section of the *xn*-evaporation reactions $\sigma_{xn}(E)$ for a given $x$, is known to have a bell-like shape with a typical width of about 6–8 MeV (for $^{48}$Ca beam energies about 240 MeV) and with a maximum at the corresponding excitation energy. Figure 6 shows the excitation functions for the nuclides produced in the reaction $^{244}$Pu + $^{48}$Ca. For the above-described isotope of element 114 (open squares), the increase in excitation energy from $E_x$ = 36 to 40 MeV results in an increase of the production cross-section from 0.5 to 2.5 pb. The further energy increase leads to the decrease of cross-section to ~1 pb at $E_x$ = 47 MeV. Finally, at $E_x$ = 53 MeV no decays of this type were detected, with the accumulated beam dose of $3 \times 10^{18}$.

At $E_x \sim 41$ MeV and at higher energies we detected also other nuclides characterized by shorter-lived decays. At $E_x = 41 \pm 2$ MeV their yield corresponded to a higher cross-section of about 5 pb. On the basis of the 12 events detected in the excitation energy interval 41–53 MeV, it follows that this nuclide emits an α-particle ($E_\alpha$ = 10.00 MeV, $T_\alpha \approx 0.6$ s) that is followed by spontaneous fission of the daughter nuclide with $T_{SF} \approx 0.1$ s. The corresponding excitation function is shown by open circles.

The data presented in Fig. 6 should be examined together with the properties of nuclei that undergo α-α-SF and α-SF decays. They differ substantially in their decay properties. Despite the small difference in the α-decay energy and half-life of the mother nuclides with $Z$ = 114, the difference in half-lives $T_\alpha$ and $T_{SF}$ of their daughters ($Z$ = 112) is definitely beyond the experimental uncertainties. Therefore, the decay chains of the two types originate from two different neighboring isotopes, which result from the evaporation of a different number of neutrons.

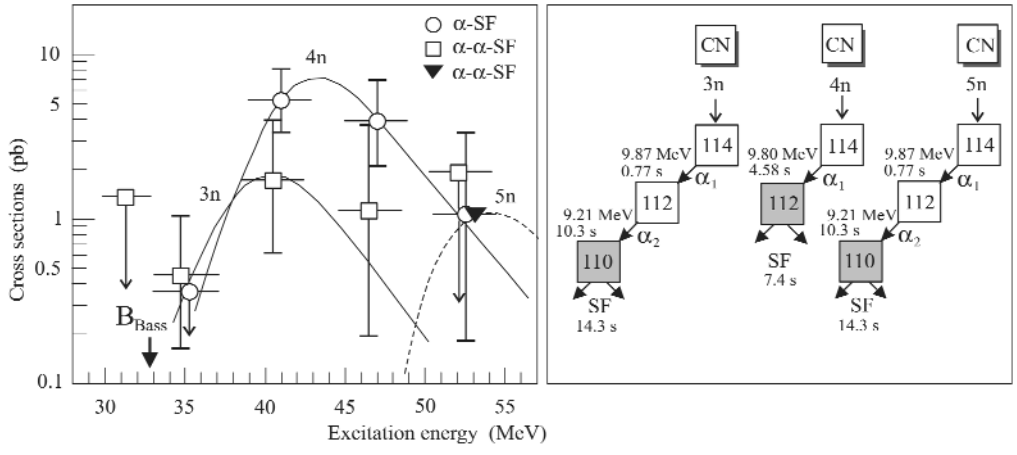


**Fig. 6** Dependence of the production cross-sections of the isotopes of element 114 on the excitation energy of the compound nucleus $^{292}$114. Lines are drawn through the experimental points to guide the eye. The right drawing shows the decay chains of the nuclei observed in the reaction $^{244}$Pu + $^{48}$Ca.

Finally, at the maximum used energy of the $^{48}$Ca ions of 253 MeV ($E_x$ = 53 MeV), we observed yet another decay chain of the α-α-SF type that differs from both that were previously described. The decay chains of all the three isotopes observed in the $^{244}$Pu + $^{48}$Ca reaction are presented in Fig. 6.

It is reasonable to consider that the short α-SF decay chains refer to the decay of the even–even nuclide $^{288}$114, the product of 4*n*-evaporation. Then the two observed α-α-SF decay sequences originate from the neighboring $^{289}$114 and $^{287}$114 isotopes, they are produced in 3*n*- and 5*n*-evaporation channels with cross-sections of about 2.7 and 1 pb, respectively.

## EXPERIMENTS ON THE SYNTHESIS OF ELEMENT 118

As stated above, the properties of the isotopes of elements 114 and 116, produced in the reactions $^{244}$Pu, $^{248}$Cm + $^{48}$Ca, are close to those calculated in the framework of the macroscopic–microscopic model. These calculations are known to predict closed nuclear shells at $Z$ = 114 and $N$ = 184 [6,7]. At the same time, in other models, such as Hartree–Fock–Bogoliubov (HFB) [18,19] or relativistic mean-field calculations (RMF) [20], the maximum shell effect for $N$ = 184 is expected at $Z$ = 120,122. Therefore, the attempt to synthesize heavier nuclei, in particular element 118, is the next logical step in studying superheavy nuclei.

Aiming at element 118 and the choice of the synthesis reaction are also motivated by the fact that we can still use $^{48}$Ca projectiles, while highly enriched $^{249}$Cf is available as a target material. The excitation energy of the $^{297}$118 compound nucleus at the Coulomb barrier of the reaction is then by 6.5 MeV lower than in the reaction $^{244}$Pu + $^{48}$Ca. Here, the maximum yield of the ERs is expected in the 2*n*- and 3*n*-evaporation channels resulting in the formation of the nuclides $^{295–294}$118. Because of the limited amount of enriched $^{249}$Cf (97.3 %) we used a 0.23-mg/cm$^2$ thick rotating target instead of the usual 0.35 mg/cm$^2$. The experiment was run from February through June 2002. In the course of the 2300-h irradiation we accumulated a total beam dose of $2.5 \times 10^{19}$ of $^{48}$Ca ions [21].

Since the decay chains of the $Z$ = 118 nuclides are expected to terminate by SF, we first searched through the data for SF events. A total of 18 SF events were detected in our experiment, see Fig. 7 for the corresponding measured summed energies. The 16 events in the lower-energy part of the spectrum ($E_{tot}$ = 125–175 MeV) originate from the decay of long-lived SF-nuclides ($T_{SF}$ > 0.5 h). These events can be ascribed to the SF of long-lived nuclides around Cf-Fm that are produced in transfer reactions. The two SF events with $E_{tot}$ > 200 MeV belong to relatively short-lived decay sequences: they are preceded by recoil signals, detected in appropriate position windows with time intervals of 0.56 s and 3.16 ms, see Fig. 7. In the first case, the recoil is followed by the emission of two alphas: the first with $E_{\alpha 1}$ = 10.65 MeV, $T_\alpha$ = 2.55 ms (in the front detector) and the second with $E_{\alpha 2}$ = 10.71 MeV, $T_{\alpha 2}$ = 42.1 ms, this one detected by both the front and side detectors. The SF with $E_{tot}$ = 207 MeV, detected as two coincident fragments, followed in 0.52 s. The probability that the 4 signals R-$\alpha_1$-$\alpha_2$-SF in this sequence are of random origin is $1.5 \times 10^{-6}$, even not taking into account that they are position-correlated.

For the second SF event, no alphas were detected in a 3.15-ms R-SF interval. Here, we also detected two coincident SF fragments with $E_{tot}$ = 223 MeV. Both events were detected at the beam energy corresponding to $E_x$ ~ 30 MeV. Here 2*n*- and 3*n*-evaporation channels are the most probable ones, leading to the formation of the isotopes of element 118 with mass numbers 295 and 294, respectively.

One cannot exclude that both decay sequences R-$\alpha_1$-$\alpha_2$-SF and R-SF represent two different decay modes of the same nuclide with $T_{1/2}$ ~ 1.8 ms produced with cross-section of about 0.7 pb. The R-$\alpha_1$-$\alpha_2$-SF chain is of special interest. If it originates from the odd nuclide $^{295}$118 (2*n*-evaporation), the two sequential α-decays should lead to the isotope $^{287}$114, which has been observed as a single event in the reaction $^{244}$Pu($^{48}$Ca,5*n*) at $E_x$ = 53 MeV. This nuclide, as one can see from Fig. 6, is an α-emitter, while the granddaughter nucleus shown in Fig. 7 undergoes SF.

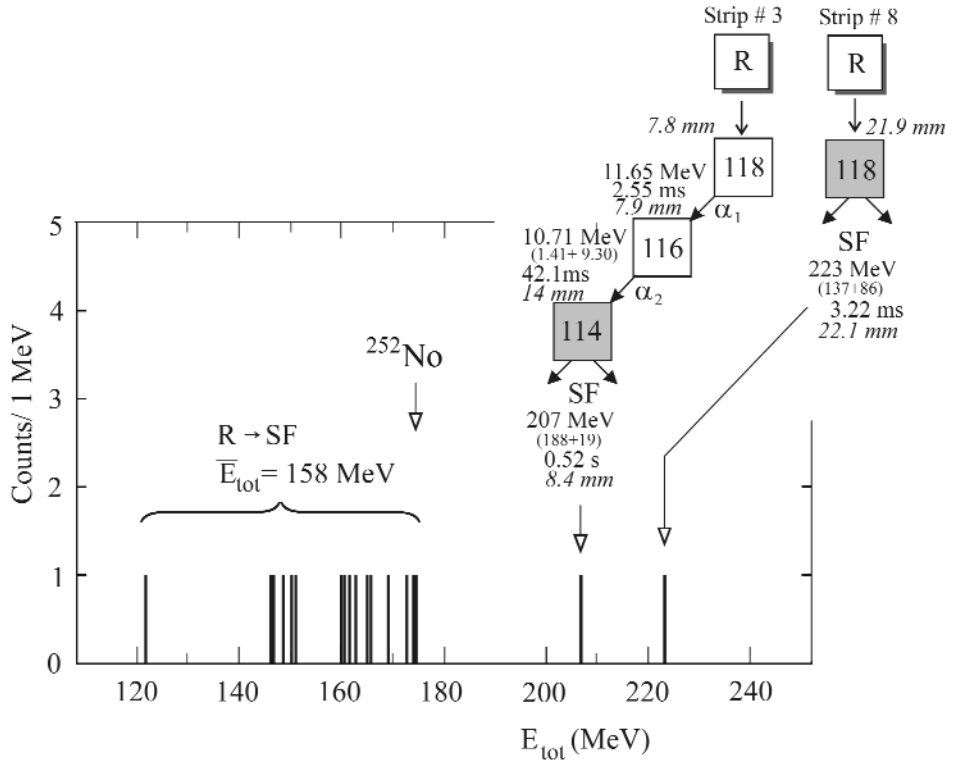


**Fig. 7** Kinetic energies of the SF fragments registered in the reaction $^{249}$Cf + $^{48}$Ca. The sum energy is given if the two fragments were detected. The decay chains are shown for the two SF events with $E_{tot}$ > 200 MeV.

However, this consideration is based only on a single event, whereas obtaining higher statistics is a difficult task because of the low production cross-sections in the discussed reactions. In these conditions, it would be useful to go a step down in $Z$, to the α-decay daughters of $Z$ = 118 nuclides, i.e., to the isotopes of element 116 with mass numbers 290 and 291. In principle, they could be synthesized with a higher yield in the reactions $^{245,246}$Cm + $^{48}$Ca.

## NEW ISOTOPES OF ELEMENT 116 PRODUCED IN THE REACTION $^{245}$Cm + $^{48}$Ca

In the experiments designed to synthesize the isotopes $^{290,\,291}$116 in the reaction $^{245}$Cm + $^{48}$Ca, we used a $^{245}$Cm target material with isotopic enrichment of 97.8 %. The beam energy in the middle of the target was set to 243 MeV, which corresponds to $E_x$ = 31–35.0 MeV close to the expected maximum yield of the 2$n$- and 3$n$-evaporation channels. In the present experiment, with the total $^{48}$Ca dose of $1.2 \times 10^{19}$ ions, we detected five decay chains of two types [22].

Two events of the first type represent two-step decay sequences (R-α-SF) with $T$ ~ 0.3–0.9 s, while the third event points to a R-α-α-SF decay pattern, see Fig. 8a. The decay pattern of the other two events differs from this type. Here, we observed the sequential emission of three α-particles that is also terminated by SF. The R-α-α-α-SF sequences last for about 10 s, their longer time duration being due to the last α-decay.

The new decay chains detected in the reaction $^{245}$Cm + $^{48}$Ca differ from the R-α-α-α-SF decays observed in the $^{248}$Cm + $^{48}$Ca reaction in energy and times of decay of the mother and daughter nuclei, see Fig. 3b. However, when comparing the daughter ($Z$ = 114) nuclei in the R-α-α-α-SF chain from the reaction $^{245}$Cm + $^{48}$Ca with the properties of the single event, detected in the $^{244}$Pu + $^{48}$Ca reaction at

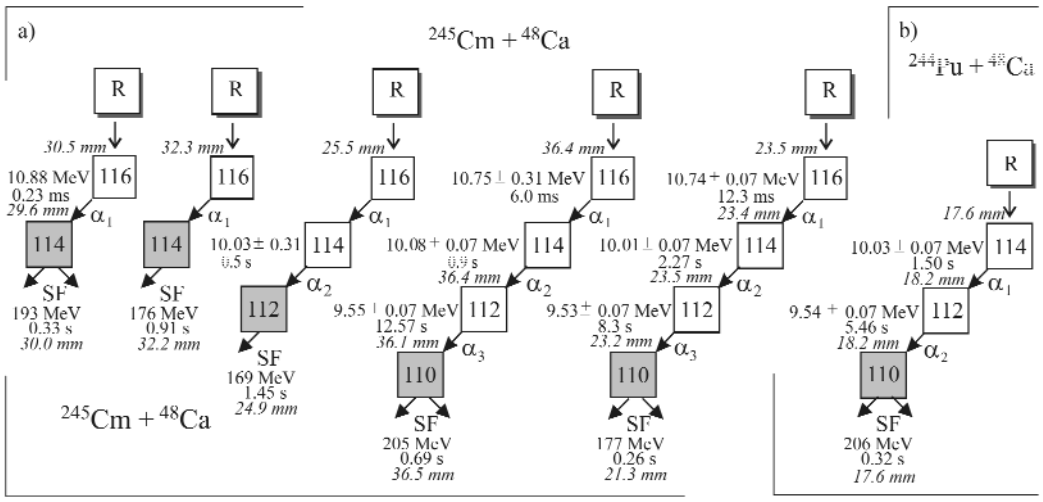


**Fig. 8** Decay chains observed in the reactions: (a) $^{245}$Cm + $^{48}$Ca at the excitation energy of the compound nucleus $^{293}$116 $E^*$ = 33 MeV and (b) $^{244}$Pu + $^{48}$Ca at $E^*$ = 53 MeV.

$E_x$ = 53 MeV and assigned to the decay of $^{287}$114, we see good agreement, Fig. 8b. Then, the longer-lived chain R-α-α-α-SF from the $^{245}$Cm + $^{48}$Ca experiment should belong to $^{291}$116, the 2*n*-evaporation product. Accordingly, the shorter-lived chain R-α-α-SF (or R-α-SF) should be assigned to the decay of the even–even nuclide $^{290}$116 produced via 3*n*-evaporation in the reaction $^{245}$Cm + $^{48}$Ca.

Now, which of these decays was observed in the experiment on the synthesis of element 118 in the reaction $^{249}$Cf + $^{48}$Ca? Most probably, the observed α-decay of the $Z$ = 118 nuclide leads to $^{290}$116. However, the decay of the primary $Z$ = 118 nuclide ends in the $Z$ = 114 granddaughter that undergoes SF with $T_{SF}$ ~ 0.5 ms. However, the α-energies of the two neighboring isotopes of element 116 with mass numbers 290 and 291 differ by just 0.1 MeV, and the α-particle energies of their descendants with $Z$ = 114 are rather close, too. One should also add here that the daughter nuclide $^{286}$114 can undergo both α-decay and SF. The real difference shows up only at $Z$ = 112: $T_\alpha$ ~ 6 s and $T_{SF}$ ~ 1 ms. Therefore, for the final identification of element 118, it is necessary to continue experiments making another step to lower $Z$ value, i.e., to isotopes with $Z$ = 114 that can be produced in the reaction $^{242}$Pu + $^{48}$Ca.

## THE REACTION $^{242}$Pu + $^{48}$Ca

This experiment is going on at present. Although it is yet not finished, the preliminary results can clarify the nuclear decay scenario. The target of enriched $^{242}$Pu (99.93 %) was irradiated with a $^{48}$Ca beam of $E$ = 244 MeV. At this energy, the compound nucleus $^{290}$114, taking into account the target thickness, has an excitation energy $E_x$ = 40 ± 2.3 MeV, for which the evaporation products of the 3*n*- and 4*n*-evaporation channels are most probable. The total beam dose was $4.7 \times 10^{18}$ ions.

In the given experiment, 10 decay chains were observed. Depending on their properties they can be subdivided into two groups (Fig. 9). The first group includes the short decays: R-SF (4 events) and R-α-SF (2 events); the total decay time in this case amounts to ~0.15 s. The spontaneous fission in the α-SF chain takes place within a very short time: $T_{SF}$ ~ 0.5 ms. These chains originate from the decay of one and the same isotope $^{286}$114, which can undergo both α-decay and SF. Its properties are in agreement with the above-mentioned decay chains of the isotope $^{290}$116, and the new events define more precisely the decay properties of the $^{286}$114 nucleus. The second group includes 4 other, longer decay chains with a long decay time. The energy of the first two α-transitions $E_{\alpha 1}$ = 10.03 MeV and $E_{\alpha 2}$ = 9.53 MeV are in agreement with the above-reported data on the decay of the $^{287}$114 isotope. As

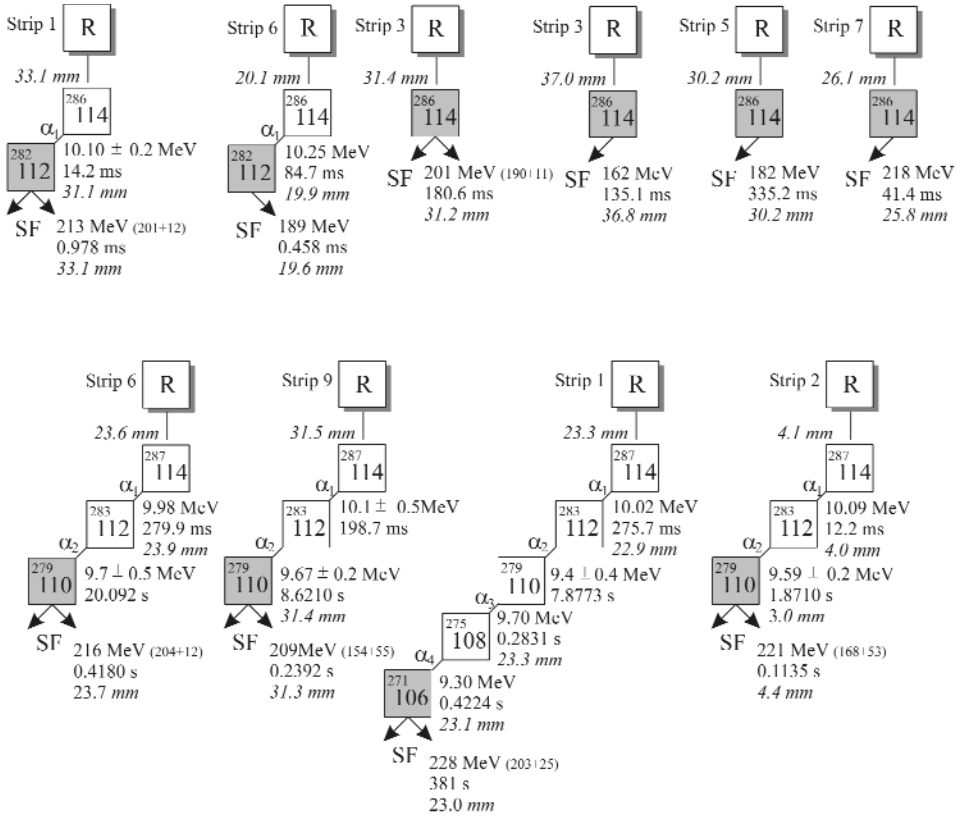


**Fig. 9** Decay chains observed in the reaction $^{242}$Pu + $^{48}$Ca at the excitation energy of the compound nucleus $^{290}$114 $E^*$ = 40 MeV.

in the previous cases, here 3 out of the 4 events consist of 2 α-decays terminating by SF with $T_{SF}$ ~ 0.2 s. In one case, spontaneous fission competes with α-decay. This leads to a longer decay chain R-$\alpha_1$-$\alpha_2$-$\alpha_3$-$\alpha_4$-SF. The final nucleus in this chain, as we suppose it to be $^{271}$Sg, fissions spontaneously for $T_{SF}$ = 381 s. It should be noted that spontaneous fission of the neutron-rich nucleus with $Z$ = 106 and $N$ = 165 is characterized by a high fission fragment kinetic energy: $E_{tot}$ = 228 MeV.

Thus, two isotopes of element 114 with mass numbers 287 and 286, formed in the 3$n$- and 4$n$-evaporation channels, have been observed in the $^{242}$Pu + $^{48}$Ca reaction at $E_x$ = 40 MeV. For an additional confirmation of this conclusion, we plan to measure their excitation functions in the $^{242}$Pu + $^{48}$Ca reaction.

However, it is possible on the basis of the already obtained data to create a picture of the decay pattern of the isotopes $^{294}$118 and $^{295}$118. In the decay of the even–even isotope $^{294}$118 (3$n$-channel) a decay chain R-$\alpha_1$-$\alpha_2$-SF is expected. As mentioned above, this chain was observed in the first $^{249}$Cf + $^{48}$Ca experiment. In about 30 % of the cases a chain of the type R-$\alpha_1$-$\alpha_2$-$\alpha_3$-SF is expected also. In the decay of the neighboring even–odd nuclide $^{295}$118 (2$n$-channel), a longer decay chain R-$\alpha_1$-$\alpha_2$-$\alpha_3$-$\alpha_4$-SF is expected; with probability of ~10 % this decay may lead to the SF nuclide, $^{271}$Sg.

In conclusion, we can say that for the daughter nuclei, the isotopes $^{290,291}$116, both the pattern of their decay and the basic decay characteristics have been determined: energies, α-transition times, and SF lifetimes. The next experiment aimed at the synthesis of element 118 is planned for the year 2004.

## EXPERIMENTS ON THE SYNTHESIS OF ODD-*Z* NUCLEI IN THE $^{243}$Am($^{48}$Ca,*xn*)$^{291-x}$115 REACTION

Our previous experiments were aimed at the synthesis of even-*Z* superheavy elements (114–118) in $^{48}$Ca-induced reactions. For the odd-*Z* elements, especially their odd–odd isotopes, the probability of α-decay with respect to SF should increase due to hindrance for SF. For such odd-*Z* nuclei, one might expect longer sequences of α-decay terminated by SF of relatively light descendant nuclides ($Z \leq 105$).

The decay pattern of these superheavy nuclei is of interest for nuclear theory. In the course of α-decays, the increased stability of nuclei, caused by the predicted spherical neutron shell $N = 184$ (or perhaps sub-shell $N = 172$), should gradually become weaker for descendant isotopes. However, the stability of these nuclei at the end of the decay chains should increase again due to the influence of the deformed shell at $N = 162$. The observation of nuclei passing from spherical to deformed shapes could provide valuable information about the influence of the changes in nuclear structure on the decay properties of nuclei. For these investigations, we chose the fusion-evaporation reaction $^{243}$Am + $^{48}$Ca, leading to isotopes of element 115.

According to calculations based on the results of experiments on the synthesis of even-*Z* nuclei [22], the 3*n*- and 4*n*-evaporation channels leading to the isotopes $^{288}$115 ($N = 173$) and $^{287}$115 ($N = 172$) should be observed with the highest yields.

The experiments were performed from 14 July until 10 August 2003. Over this period, equal beam doses of $4.3 \times 10^{18}$ were delivered to the target at two bombarding energies for the $^{48}$Ca ions of 248 and 253 MeV. With the beam energy resolution and energy losses in the target (~3.3 MeV), we expected the resulting compound nuclei $^{291}$115 to have excitation energies of 38.0–42.3 and 42.4–46.5 MeV, respectively [23].

The three similar decay chains observed at 248 MeV are shown in Fig. 10a. The implantations of recoils in the focal-plane detector were followed by α-particles with $E_\alpha = 10.46 \pm 0.06$ MeV. These sequences switched the ion beam off, and four more α-decays were detected in time intervals of 29, 15, and 20 s, respectively, in the absence of beam-associated background. During the remainder of the 2.5-h beam-off period following the last position-correlated α-particle, no α-particles with $E_\alpha > 7.6$ MeV were registered by the focal-plane detectors. The spontaneous fission of the final nuclei in these chains was detected 28.7, 23.5, and 16.8 h, respectively, after the last α-decay. A search was performed to identify α-decays correlated closely in time (<60 s) and position to each of the three SF events in Fig. 10a. No correlations were found.

In the first two decay chains, the front and side detectors simultaneously detected fission fragments with sum energies of 205 and 200 MeV. In the third chain, only the front detector registered a fission fragment. All three SF events were registered in the corresponding strips and positions where the three R-$\alpha_1$-...-$\alpha_5$ decay chains were observed. Thus, these SF events should be assigned to the spontaneous fission of the descendant nuclei in these observed chains. At 253 MeV, the aforementioned R-$\alpha_1$-...-$\alpha_5$-SF decay chains were not observed. However, a different decay chain, consisting of four α-decays and spontaneous fission, was registered (see Fig. 10b). The beam was switched off after the detection of an R-signal followed in 46.6 ms by an α-particle with $E_\alpha = 10.50$ MeV in the same position of strip 7. Three other α-decays were detected in a time interval of about 0.4 s in the absence of beam-associated background. After 106 min, the terminating SF event was detected in-beam with a sum energy of 206 MeV in the same position of the strip 7. A more detailed description of the data analysis is given in our paper [23].

The radioactive properties of nuclei in this decay chain differ from those of the nuclei observed at the lower bombarding energy. The total decay time of this chain is about 10 times shorter and the α-decays are distinguished by higher α-particle energies and shorter lifetimes. Its production required also increasing the beam energy by about 5 MeV, so this decay chain must originate from another parent nucleus.

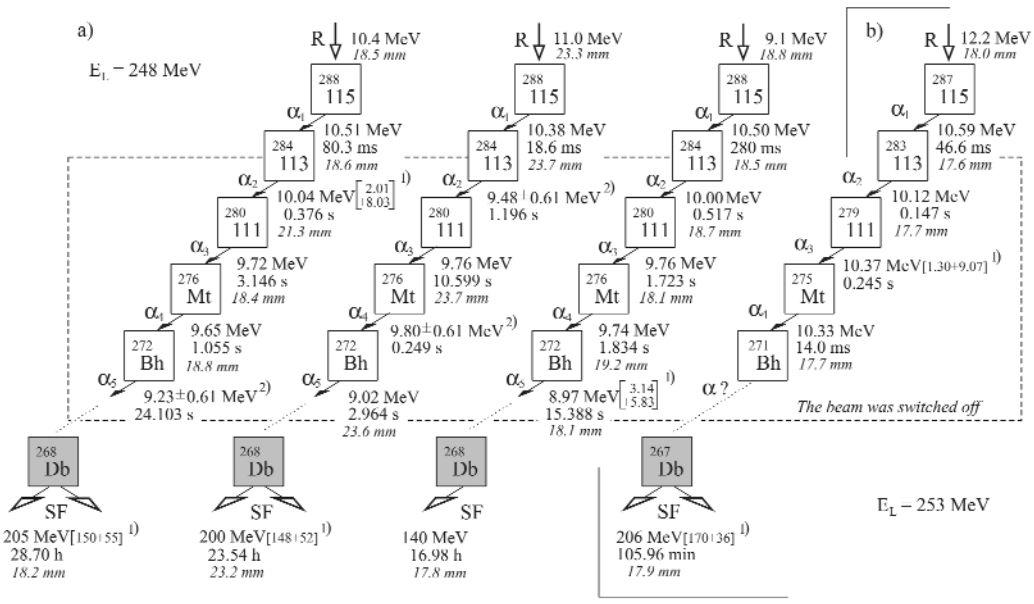


**Fig. 10** Time sequences in the decay chains observed in the $^{243}$Am + $^{48}$Ca reaction at two $^{48}$Ca energies: (a) $E_L$ = 248 MeV and (b) $E_L$ = 253 MeV. Measured energies, time intervals, and positions of the observed decay events are shown. (1) Energies of events detected by both the front and side detectors. (2) Energies of events detected by side detectors only. We have inserted an unobserved nuclide in the fourth decay chain.

It is most probable that the different decay chains originate from neighboring parent isotopes of element 115, produced in the complete fusion reaction $^{243}$Am + $^{48}$Ca followed by evaporation of three and four neutrons from the compound nucleus $^{291}$115. Indeed, at the excitation energy $E_x$ = 40 MeV, close to the expected maximum for the 3*n*-evaporation channel, we observed longer decay chains of the odd–odd isotope $^{288}$115. Increasing the beam energy by 5 MeV results in reducing the $^{288}$115-isotope yield and, at the same time, increasing the yield of the 4*n*-evaporation channel leading to the even–odd isotope $^{287}$115. Corresponding cross-sections for the 3*n*- and 4*n*-evaporation channels at the two projectile energies were measured to be $\sigma_{3n}$ ~ 2.7 pb and $\sigma_{4n}$ ~ 0.9 pb.

In the decay chains shown in Fig. 10a, we assigned SF events to the isotope $^{268}$Db following five consecutive α-decays. This isotope has also the possibility of undergoing α-decay or electron capture (EC). In the case of the α-decay of $^{268}$Db with $T_\alpha$ > 2.5 h (after the beam-off period), one would more reasonably expect SF or EC of $^{264}$Lr, because the α-decay of $^{264}$Lr seems improbable due to the expected low α-decay energy ($Q_\alpha$ = 6.84 MeV [24], $T_\alpha$ > 100 d). The electron capture of $^{268}$Db or $^{264}$Lr leads to the even–even isotopes $^{268}$Rf or $^{264}$No, for which fast spontaneous fission can be expected (e.g., $T_{SF}$ = 1.4 s is predicted for $^{268}$Rf [25]). Since both fission fragments of these final nuclei can have the $Z$ = 50 and $N$ = 82 closed-shell configurations, one would expect their SF-decays to result in narrow symmetric mass distributions with rather high TKEs ≈ 230–240 MeV (see, e.g., ref. [26]). Indeed, the sum fission fragment energies observed for the final nuclei are close to this value. It is noteworthy that the likelihood that EC-decay occurs earlier in the observed decay chains is small because of the short $T_\alpha$ for the observed α-decays of elements 115, 113, 111, Mt, and Bh.

In the decay chain originating from $^{287}$115 (see Fig. 10b), it seems that we must have missed the α-decay of $^{271}$Bh. The expected $T_\alpha$ value for $^{271}$Bh should be ~10 s ($Q_\alpha$ = 9.07 MeV [12]), which is much shorter than the interval between the last observed α-particle and the terminating SF event, but is much longer than the intervals between the observed correlated α-particles. Such a decay scheme of $^{287}$115 is also supported by the agreement of the observed decay properties of the other nuclides in the

decay chains with the expectations of theory. This means that SF occurs directly in the decay of $^{267}$Db since the calculated α-decay and EC-energies for this isotope are rather low ($Q_\alpha$ = 7.41 MeV, $Q_{EC}$ = 1 MeV) and their expected partial half-lives significantly exceed the observed time interval of 106 min.

## THEORY AND EXPERIMENT

From the recent experimental results given in the present paper, together with already available data, we can get an idea of the current state of the problem of the synthesis of superheavy elements and outline our future plans.

The formation and decay of four isotopes of element 114 with atomic masses 286–289 and three isotopes of element 116 with masses 290, 291, and 293 were observed in the reactions $^{242,244}$Pu, $^{245,248}$Cm + $^{48}$Ca. All these nuclei predominantly undergo a series of α-decays, which finally terminate by spontaneous fission. In the chains of the even–even isotopes $^{286,288}$114 spontaneous fission is observed in the daughter nuclei ($Z$ = 112); the isotope $^{286}$114, together with α-decay, with high probability undergoes spontaneous fission, too. Such a decay pattern is in good agreement with theoretical predictions.

From the events from which both fission fragments were detected, we can estimate the TKE in the SF of the new nuclides without claiming high accuracy of these figures because of the small number of detected events and the necessity of involving corrections for losses in the measured fragment energies (Fig. 11). Our experimental data point to asymmetric mass division in the spontaneous fission of the heaviest nuclei that is in agreement with the data on mass distributions in fission of the excited

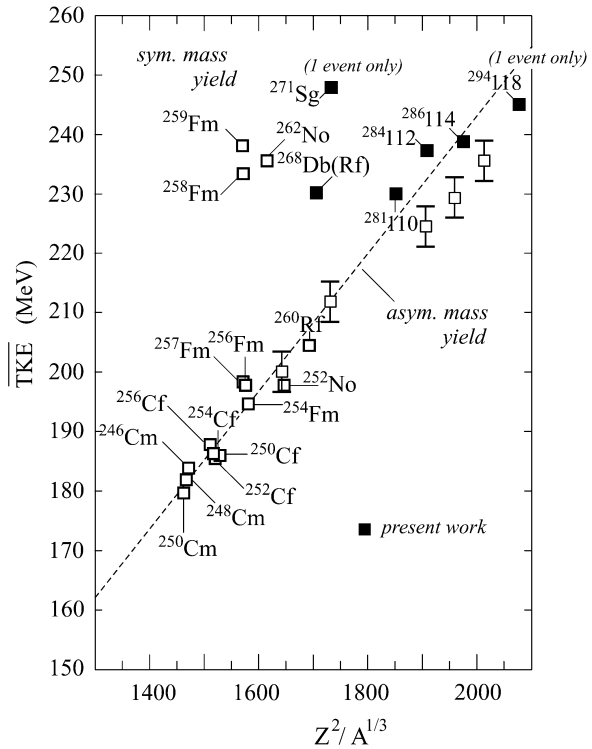


**Fig. 11** Mean TKE of fission fragments vs. the parameter $Z^2/A^{1/3}$ for the spontaneous fission of the nuclides with $Z$ = 96–118. Open squares present literature data; full squares present the SF detected in the decay chains of the superheavy nuclides (see text).

nuclei with $E^*$ ~ 30–40 MeV [27]. On the contrary, in the long decay chains of the odd-$Z$ nuclei (not excluded also for even–odd isotopes) the high value of TKE is most probably connected with the symmetric fission mode of deformed nuclei ($Z$ ~ 104–106, $N \geq 162$) due to the effect of the spherical shells $Z = 50$ and $N = 82$ in the fission fragments.

Alpha-transitions in the decay chains of $Z = 114$, 116 isotopes have well-defined energies pointing to the absence of hindrance in the observed decays that is characteristic of the α-decay of spherical nuclei. For odd-$Z$ isotopes, the measured $T_\alpha$ values closely reproduce the calculated ones for the first two nuclei of these chains, too. The observed isotopes with $Z = 113$, 115 have rather low hindrance factors, if any, for α-decay. For the isotopes of elements 111, Mt and Bh, the difference between measured and calculated $T_\alpha$ values results in hindrance factors of 3–10.

The energies $Q_\alpha$ and half-lives $T_\alpha$ of the even-Z nuclides with $Z \geq 108$ are presented in Figs. 12a and 12b together with the calculations made within the macroscopic–microscopic model. The available experimental data is in general agreement with the theoretically predicted considerable enhancement of nuclear stability in the vicinity of the deformed shells $Z = 108$ and $N = 162$. For the isotopes with $Z = 112$–116 and $N \geq 170$, the expected increase of nuclear stability due to the effect of the spherical $N = 184$ shell is also clearly observed. Experimental $Q_\alpha$ values of the isotopes with $Z = 110$–116 are by 0.1–0.5 MeV lower than the calculated values. Correspondingly, their half-lives are 2 to 10 times longer than theoretically predicted.

It is interesting to know what is the longest possible lifetime of nuclei in the new region of stability of superheavy elements. Getting an answer to such a question is not easy, because the synthesis of very neutron-rich ($N$ ~ 180–184) nuclides is a difficult task due to limitations imposed by the proton-to-neutron ratio in the target and projectile nuclei. But if their lifetimes are longer than $10^8$ years, they may have survived in natural samples since the moment of nucleosynthesis until now.

In 1969–1989, at different laboratories in Berkeley (USA) [28], Mainz (Germany) [29], Orsay (France) [30], and Dubna [31] experiments were carried out to search for superheavy elements in natural samples. At that time, the concept of the experiments and choice of objects were based on the assumption that the nuclide with $Z = 114$ was considered to be the most stable one ($T_{1/2} \geq 10^8$ yr). However, the calculations, describing our experimental data on the isotopes of element 114 with neutron numbers $N = 172$–175, predict for the nucleus with $Z = 114$ and $N = 184$ a lifetime by 12 orders of magnitude shorter ($T_\alpha$ ~$10^3$ s).

The most stable nucleus is determined by the probability (or partial half-life) to undergo α- and β-decays and spontaneous fission. Unfortunately, the calculated $T_\alpha$ values vary strongly in different nuclear models. The calculated SF probabilities may differ by 4–5 orders of magnitude even for a specified configuration of the barrier. On the other hand, the heights of the fission barriers for nuclei with specified values of $Z$ and $N$ are scattered within a range of several MeV, which also changes $T_{SF}$ by several orders. In such a situation, the extrapolation of known experimental values of $T_{SF}$ and $T_\alpha$ into the region of $N = 178$–184 leads us to the nuclei of element 108 lying on or in the vicinity of the β-stability line ($N = 178$–180).

The half-life of these nuclei should be $T_{1/2} \geq 3.10^{15}$ s (~$10^8$ yr) in order to be observed in small quantities in earth samples. Since at present there are no direct arguments in favor of the existence of SHE in nature, the experiment on the search for extremely long-lived isotopes of element 108 is motivated solely by the mere assumption that *it cannot be excluded*.

It is assumed that long-lived nuclides undergo α- and β-decay or spontaneous fission. In the case of sequential α- and β-decays, the finite nuclei will undergo spontaneous fission. As a first step, it is proposed to search in an Os sample for its chemical homologue EkaOs [32] by means of measuring multiple neutron emission accompanying spontaneous fission.

A neutron detector which is now being manufactured at JINR will be capable with an efficiency of ~50 % to register rare events of spontaneous fission of superheavy nuclei in the form of three and more coincidences of signals arising from 60 $^3$He-neutron detectors surrounding the examined sample.

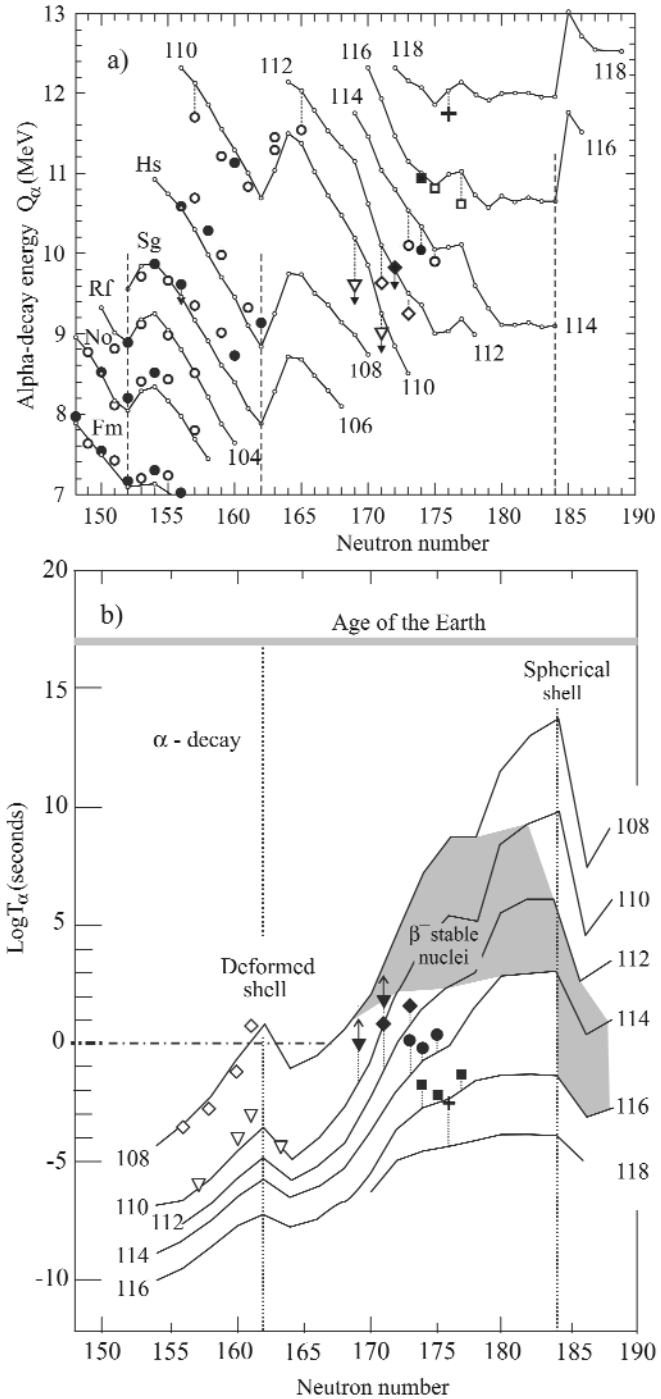


**Fig. 12** (a) Decay energy $Q_\alpha$ of the even-$Z$ isotopes with $Z$ = 100–118 vs. neutron number. Full symbols show data for even–even nuclei; open symbols for even–odd ones. Data for $Z$ = 110–118 and $N \geq 170$ are from experiments with $^{48}$Ca projectiles. (b) Half-lives Log($T_\alpha$) for the nuclei with $Z$ = 108–118 vs. neutron number. Solid lines present the calculations in the macroscopic-microscopic model [6,7]. Dashed lines indicate the closed neutron shells $N$ = 152, 162, and 184.

The expected background of multiple production of neutrons imitating spontaneous fission of the superheavy nucleus in the Underground Laboratory (Modane, France) is ≤0.1/yr. For an Os sample, 500 g in weight, the registration of one event of spontaneous fission per year will correspond to a concentration of the superheavy nuclide at the level of ~$5.10^{-15}$ g/g assuming that its half-life is $T_{1/2} \sim 10^9$ yr. Correspondingly, non-observation of spontaneous fission in this experiment will yield an upper limit of the average concentration of long-lived atoms of element 108 at the level of $10^{-22}$ g/g assuming $T_{1/2} \approx 10^9$ yr. This quantity is ~$10^{-16}$ less than the abundance of $^{238}$U in the Earth's crust.

## ACKNOWLEDGMENTS

The experiments were carried out at the heavy ion cyclotron U400 of the Flerov Laboratory of Nuclear Reactions JINR (Dubna) in collaboration with the Analytical and Nuclear Chemistry Division of LLNL (Livermore).

The significant contribution of my colleagues and coauthors from FLNR: V. K. Utyonkov, Yu. V. Lobanov, F. Sh. Abdullin, A. N. Polyakov, I. V. Shirokovsky, Yu. S. Tsyganov, A. N. Mezentsev, M. G. Itkis, during all stages of the preparation and performing this research together with our collaborators: K. J. Moody, J. B. Patin, J. F. Wild, M. A. Stoyer, N. J. Stoyer and R. W. Lougheed from LLNL, is gratefully acknowledged.

We are grateful to G. G. Gulbekian and the staff of the accelerator department for producing the intense $^{48}$Ca beams, and also to V. I. Zagrebaev and S. N. Dmitriev for their assistance in performing this work.

In the experiments we used targets made of unique materials—isotopes of Pu, Am, Cm and Cf, produced at the high flux reactors at Dimitrovgrad (Russia), Oak Ridge (USA), and enriched with the mass-separator S2 in Sarov (Russia). We are greatly indebted to our colleagues who have performed the very difficult job of preparing the targets.

This work has been performed with the support of the Russian Ministry of Atomic Energy and grants of RFBR No. 01-02-16486, 03-02-06236 and 04-02-17186. Much of the support for the LLNL authors was provided through the U.S. DOE under Contract No. W-7405-Eng-48.

Finally, I would also like to thank the Programme Committee and personally acad. O. M. Nefedov and N. A. Plate for the invitation to give this talk.

## REFERENCES

1. G. N. Flerov and K. A. Petrzhak. *Phys. Rev.* **58**, 89 (1940); *J. Phys. (Moscow)* **3**, 275 (1940).
2. N. Bohr and J. A. Wheeller. *Phys. Rev.* **56**, 426 (1939).
3. S. M. Polikanov, V. A. Druin, V. A. Karnaukhov, V. L. Mikheev, A. A. Pleve, N. K. Skobelev, G. M. Ter-Akopyan, V. A. Fomichev. *Zh. Sov. Phys.* JETP **15**, 1016 (1962).
4. S. Bjornholm and J. Linn. *Rev. Mod. Phys.* **52**, 725 (1980).
5. Yu. Ts. Oganessian, A. G. Demin, A. S. Iljinov, S. P. Tretyakova, A. A. Pleve, Yu. E. Penionzhkevich, M. P. Ivanov, Yu. P. Tretyakov. *Nucl. Phys. A* **239**, 157 (1975).
6. Z. Patyk and A. Sobiczewski. *Nucl. Phys. A* **533**, 132 (1991).
7. R. Smolanczuk. *Phys. Rev. C* **56**, 812 (1997).
8. G. T. Seaborg. *Man-Made Transuranium Elements*, Prentice Hall, New York (1963).
9. Yu. Ts. Oganessian. *Lect. Notes Phys.* **33**, 221 (1974).
10. S. Hofmann. *On Beyond Uranium*, V. Moses (Ed.), Taylor & Francis, London (2002).
11. E. K. Hulet, R. W. Lougheed, J. F. Wild, J. H. Landrum, P. C. Stevenson, A. Ghiorso, J. M. Nitschke, R. J. Otto, D. J. Morrissey, P. A. Baisden, B. F. Gavin, D. Lee, R. J. Silva, M. M. Fowler, G. T. Seaborg. *Phys. Rev. Lett.* **39**, 385 (1977).

12. Yu. Ts. Oganessian, H. Bruchertseifer, G. V. Buklanov, V. I. Chepigin, Choi Val Sek, B. Eichler, K. A. Gavrilov, H. Gaeggeler, Yu. S. Korotkin, O. A. Orlova, T. Reetz, W. Seidel, G. M. Ter-Akopian, S. P. Tretyakova. *Nucl. Phys. A* **294**, 213 (1978).
13. P. Armbruster, Y. K. Agarwal, W. Brüchle, M. Brügger, J. P. Dufour, H. W. Gäggeler, F. P. Hessberger, S. Hofmann, P. Lemmertz, G. Münzenberg, K. Poppensieker, W. Reisdorf, M. Schädel, K.-H. Schmidt, J. H. R. Schneider, W. F. W. Schneider, K. Sümmerer, D. Vermeulen, G. Wirth, A. Ghiorso, K. E. Gregorich, D. Lee, M. Leino, K. J. Moody, G. T. Seaborg, R. B. Welch, P. Wilmarth, S. Yashita, C. Frink, N. Greulich, G. Herrmann, U. Hickmann, N. Heidebrand, J. V. Kratz, N. Trautmann, M. M. Fowler, D. C. Hoffman, W. R. Daniels, H. R. von Gunten, H. Dornhöfer. *Phys. Rev. Lett.* **54**, 406 (1985).
14. K. Subotic, Yu. Ts. Oganessian, V. K. Utyonkov, Yu. V. Lobanov, F. Sh. Abdullin, A. N. Polyakov, Yu. S. Tsyganov, O. V. Ivanov. *Nucl. Instr. Meth. Phys. Res. A* **481**, 71 (2002).
15. Yu. Ts. Oganessian, V. K. Utyonkov, Yu. V. Lobanov, F. Sh. Abdullin, A. N. Polyakov, I. V. Shirokovsky, Yu. S. Tsyganov, G. G. Gulbekian, S. L. Bogomolov, B. N. Gikal, A. N. Mezentsev, S. Iliev, V. G. Subbotin, A. M. Sukhov, O. V. Ivanov, G. V. Buklanov, K. Subotic, M. G. Itkis, K. J. Moody, J. F. Wild, N. J. Stoyer, M. A. Stoyer, R. W. Lougheed. *Phys. Rev. C* **62**, 041604(R) (2000); *Phys. At. Nucl.* **63**, 1679 (2000).
16. Yu. Ts. Oganessian, V. K. Utyonkov, Yu. V. Lobanov, F. Sh. Abdullin, A. N. Polyakov, I. V. Shirokovsky, Yu. S. Tsyganov, G. G. Gulbekian, S. L. Bogomolov, B. N. Gikal, A. N. Mezentsev, S. Iliev, V. G. Subbotin, A. M. Sukhov, O. V. Ivanov, G. V. Buklanov, K. Subotic, M. G. Itkis, K. J. Moody, J. F. Wild, N. J. Stoyer, M. A. Stoyer, R. W. Lougheed, C. A. Laue, Ye. A. Karelin, A. N. Tatarinov. *Phys. Rev. C* **63**, 011301(R) (2001); Yu. Ts. Oganessian, V. K. Utyonkov, K. J. Moody. *Phys. At. Nucl.* **64**, 1349 (2001); Yu. Ts. Oganessian, V. K. Utyonkov, Yu. V. Lobanov, F. Sh. Abdullin, A. N. Polyakov, I. V. Shirokovsky, Yu. S. Tsyganov, G. G. Gulbekian, S. L. Bogomolov, B. N. Gikal, A. N. Mezentsev, S. Iliev, V. G. Subbotin, A. M. Sukhov, O. V. Ivanov, G. V. Buklanov, K. Subotic, A. A. Voinov, M. G. Itkis, K. J. Moody, J. F. Wild, N. J. Stoyer, M. A. Stoyer, R. W. Lougheed, C. A. Laue. *Eur. Phys. J. A* **15**, 201 (2002).
17. V. E. Viola, Jr. and G. T. Seaborg. *J. Inorg. Nucl. Chem.* **28**, 741 (1966).
18. S. Ćwiok, W. Nazarewicz, P. H. Heenen. *Phys. Rev. Lett.* **83**, 1108 (1999).
19. S. Typel and B. A. Brown. *Phys. Rev. C* **67**, 034313 (2003).
20. M. Bender. *Phys. Rev. C* **61**, 031302 (2000); P.-G. Reinhard, M. Bender, T. Bürvenich, T. Cornelius, P. Fleischer, J. A. Maruhn, in *Proc. Tours Symposium on Nuclear Physics IV*, Tours, France, 2000 (AIP, New York, 2001), p. 377; Z. Ren. *Phys. Rev. C* **65**, 051304(R) (2002).
21. Yu. Ts. Oganessian, V. K. Utyonkov, Yu. V. Lobanov, F. Sh. Abdullin, A. N. Polyakov, I. V. Shirokovsky, Yu. S. Tsyganov, A. N. Mezentsev, S. Iliev, V. G. Subbotin, A. M. Sukhov, O. V. Ivanov, A. A. Voinov, K. Subotic, V. I. Zagrebaev, M. G. Itkis, K. J. Moody, J. F. Wild, M. A. Stoyer, N. J. Stoyer, C. A. Laue, D. A. Shaughnessy, J. B. Patin, R. W. Lougheed. Communication of the Joint Institute for Nuclear Research, D7-2002-287, Dubna, 2002.
22. Yu. Ts. Oganessian, V. K. Utyonkov, Yu. V. Lobanov, F. Sh. Abdullin, A. N. Polyakov, I. V. Shirokovsky, Yu. S. Tsyganov, G. G. Gulbekian, S. L. Bogomolov, B. N. Gikal, A. N. Mezentsev, S. Iliev, V. G. Subbotin, A. M. Sukhov, A. A. Voinov, G. V. Buklanov, K. Subotic, V. I. Zagrebaev, M. G. Itkis, J. B. Patin, K. J. Moody, J. F. Wild, M. A. Stoyer, N. J. Stoyer, D. A. Shaughnessy, J. M. Kenneally, R. W. Lougheed. *Phys. Rev. C*. **69**, 054607 (2004).
23. Yu. Ts. Oganessian, V. K. Utyonkov, Yu. V. Lobanov, F. Sh. Abdullin, A. N. Polyakov, I. V. Shirokovsky, Yu. S. Tsyganov, G. G. Gulbekian, S. L. Bogomolov, A. N. Mezentsev, S. Iliev, V. G. Subbotin, A. M. Sukhov, A. A. Voinov, G. V. Buklanov, K. Subotic, V. I. Zagrebaev, M. G. Itkis, J. B. Patin, K. J. Moody, J. F. Wild, M. A. Stoyer, N. J. Stoyer, D. A. Shaughnessy, J. M. Kenneally, R. W. Lougheed. *Phys. Rev*. *C* **69**, 021601(R) (2004).
24. I. Muntian, S. Hofmann, Z. Patyk, A. Sobiczewski. *Acta Phys. Pol. B* **34**, 2073 (2003); I. Muntian, Z. Patyk, A. Sobiczewski. *Phys. At. Nucl.* **66**, 1015 (2003).

25. R. Smolańczuk, J. Skalski, A. Sobiczewski. *Phys. Rev. C* **52**, 1871 (1995).
26. D. C. Hoffman and M. R. Lane. *Radiochim. Acta* **70/71**, 135 (1995).
27. M. G. Itkis, A. A. Bogatchev, I. M. Itkis, M. Jandel, G. N. Kniajeva, N. A. Kondratiev, I. V. Korzyukov, E. M. Kozulin, L. Krupa, Yu. Ts. Oganessian, I. V. Pokrovski, V. A. Ponomarenko, E. V. Prokhorova, A. Ya. Rusanov, V. M. Voskresenski, A. A. Goverdovski, F. Hanappe, T. Materna, N. Rowley, L. Stuttge, G. Giardina, K. J. Moody. *J. Nucl. Radiochem. Sci.* **3**, 57 (2002); in *Proceedings of the Second International Conference on Fission and Properties of Neutron-Rich Nuclei*, St. Andrews, Scotland, 1999, p. 268, World Scientific, Singapore.
28. E. Cheifetz, R. C. Jared, E. R. Guisti, S. G. Thompson. *Phys. Rev. C* **6**, 1348 (1972); R. W. Stoughton, J. S. Drury, R. J. Silva, M. H. Leitzke, J. Halperin, R. C. Jared, S. G. Thompson, E. R. Guisti, E. Cheifetz. *J. Inorg. Nucl. Chem. Suppl.* **215** (1976).
29. H.-J. Becker, R. Brandt, H. Junglas, T. Lund, D. Molzan. *Nucl. Instrum. Meth.* **159**, 75 (1979); R. A. Esterlund, D. Molzan, R. Brandt, P. Patzelt, P. Vater, A. H. Boos, M. R. Chandratillake, I. S. Grant, I. D. Hemingway, G. W. A. Newton. *Phys. Rev. C* **15**, 319 (1977).
30. C. Stephan, M. Epherre, E. Cieslak, M. Sowinsky, J. Tys. *Phys. Rev. Lett.* **37**, 1534 (1974); M. Epherre and R. Klapisch. *Phys. Rev. C* **13**, 206 (1976).
31. G. N. Flerov and G. M. Ter-Akopian. In *Treatise on Heavy–Ion Science*, Vol. 4, Extreme Nuclear States, D. A. Bromley (Ed.), p. 333, Plenum Press, New York (1985).
32. Ch. E. Düllmann, W. Brüchle, R. Dressler, K. Eberhardt, B. Eichler, R. Eichler, H. W. Gäggeler, T. N. Ginter, F. Glaus, K. E. Gregorich, D. C. Hoffman, E. Jäger, D. T. Jost, U. W. Kirbach, D. M. Lee, H. Nitsche, J. B. Patin, V. Pershina, D. Piguet, Z. Qin, M. Schädel, B. Schausten, E. Schimpf, H.-J. Schött, S. Soverna, R. Sudowe, P. Thörle, S. N. Timokhin, N. Trautmann, A. Türler, A. Vahle, G. Wirth, A. B. Yakushev, P. M. Zielinski. *Nature* **418**, 859 (2002).

## NOTE ADDED IN PROOF

By July 2004, the data presented in the talk were confirmed and complemented by the results of the new experiments including the chemical identification of $^{268}$Db—the final decay product of the isotope $^{288}$115. The updated record of radioactive properties of the new isotopes and their decay products is given in the Table.

| Z | A | No. events | Decay mode | Half-life | $Q_\alpha$ MeV | Z | A | No. events | Decay mode | Half-life | $Q_\alpha$ MeV | Z | A | No. events | Decay mode | Half-life | $Q_\alpha$ MeV |
|---|---|---|---|---|---|---|---|---|---|---|---|---|---|---|---|---|---|
| 118 | 294 | 1 | α/SF | 1.8 ms | 11.81 | 114 | 286 | 11 | α/SF | 0.16 s | 10.35 | 110 | 279 | 21 | SF/α | 0.18 s | 9.84 |
| 116 | 293 | 4 | α | 61 ms | 10.69 | 113 | 284 | 3 | α | 0.48 s | 10.15 | 109 | 276 | 3 | α | 0.72 s | 9.85 |
| | 292 | 5 | α | 18 ms | 10.80 | | 283 | 1 | α | 0.1 s | 10.26 | | 275 | 1 | α | 9.7 ms | 10.48 |
| | 291 | 2 | α | 6.3 ms | 10.89 | 112 | 285 | 10 | α | 29 s | 9.28 | 108 | 275 | 2 | α | 0.15 s | 9.44 |
| | 290 | 2 | α | 15 ms | 11.00 | | 284 | 17 | SF | 97 ms | ≤9.80 | 107 | 272 | 3 | α | 9.8 s | 9.15 |
| 115 | 288 | 3 | α | 87 ms | 10.61 | | 283 | 18 | α/SF | 4.0 s | 9.67 | | 271 | – | α | – | – |
| | 287 | 1 | α | 32 ms | 10.74 | | 282 | 6 | SF | 0.5 ms | ≤10.82 | 106 | 271 | 2 | α/SF | 2.4 m | 8.65 |
| 114 | 289 | 9 | α | 2.6 s | 9.96 | 111 | 280 | 3 | α | 3.6 s | 9.87 | 105 | 268 | 18 | SF/EC | 29 h | |
| | 288 | 16 | α | 0.80 s | 10.08 | | 279 | 1 | α | 0.17 s | 10.52 | | 267 | 1 | SF | 1.2 h | |
| | 287 | 15 | α | 0.51 s | 10.16 | 110 | 281 | 10 | SF | 11.1 s | ≤9.00 | 104 | 267 | 1 | SF | 2.3 h | ≤8.22 |